

The role of hydrogen in room-temperature ferromagnetism at graphite surfaces

H. Ohldag

Stanford Synchrotron Radiation Lightsource, Stanford University, Menlo Park, CA 94025, USA

P. Esquinazi

Institut für Experimentelle Physik II, Universität Leipzig, Linnéstraße 5, 04103 Leipzig, Germany

E. Arenholz

Advanced Light Source, Lawrence Berkeley National Laboratory, Berkeley, CA 94720, USA

D. Spemann, M. Rothermel, A. Setzer, T. Butz

Institut für Experimentelle Physik II, Universität Leipzig, Linnéstraße 5, 04103 Leipzig, Germany

Abstract. We present a x-ray dichroism study of graphite surfaces that addresses the origin and magnitude of ferromagnetism in metal-free carbon. We find that, in addition to carbon π states, also hydrogen-mediated electronic states exhibit a net spin polarization with significant magnetic remanence at room temperature. The observed magnetism is restricted to the top ≈ 10 nm of the irradiated sample where the actual magnetization reaches $\simeq 15$ emu/g at room temperature. We prove that the ferromagnetism found in metal-free untreated graphite is intrinsic and has a similar origin as the one found in proton bombarded graphite.

PACS numbers: 75.50.Pp, 75.30.Ds, 78.70.-g

Submitted to: *New J. Phys.*

The possibility of magnetic order in metal-free carbon is fascinating from a fundamental as well as from a technological point of view. In recent years there have been numerous reports of ferromagnetism in virgin graphite [1] as well as graphite treated by ion bombardment [2, 3, 4] and carbon nanoparticles [5, 6, 7]; it could be shown that the observed magnetism in proton irradiated carbon is not caused by magnetic impurities but is related to the π -states of carbon [8]. However, the question how it is possible to establish ferromagnetic order in carbon without any metallic magnetic or non-magnetic elements still remains unanswered. Several theoretical studies in the past have suggested that absorption of hydrogen at the edges of [9] or on [10] graphene sheets as well as hydrogen chemisorption in graphite [11] may lead to the formation of a spin polarized band at the Fermi level and robust ferromagnetic order. However, there is so far no convincing experimental evidence supporting the influence of hydrogen. While it is obvious that defects or ad-atoms play a central role, the origin of the magnetic moment observed in graphite [1] is not yet understood.

Another intriguing question arises from the observation that the apparent magnetization detected in magnetic graphite is typically many orders of magnitude smaller than the one found for “classical” magnets like the 3d-transition metals. Apart from the fact that this makes it challenging to obtain a reliable and detailed understanding of the relevant processes that cause the ferromagnetic order in graphite [12], it also leads to the question how such a system exhibiting a small magnetization and presumably negligible magnetic exchange coupling can be a ferromagnet at room temperature. However, the explanation of such extremely small magnetization resides in the uncertainty of the total ferromagnetic mass in the measured samples and in the role of non-metallic defects. Recent studies on proton- [3] and carbon-irradiated [4] graphite managed to provide maximum limits for the induced ferromagnetic mass allowing to estimate magnetization values exceeding 5 emu/g. Although important evidence has been obtained that supports the role of vacancies in the graphite ferromagnetism [13], the very origin and extent of surface magnetism [14] remains open. For this reason we will investigate the electronic structure of such samples and correlate our findings with the macroscopic magnetic properties.

In this paper we present x-ray absorption (XA) and x-ray magnetic circular dichroism (XMCD) spectra in combination with Superconducting Quantum Interference Device (SQUID) measurements on proton irradiated and non-irradiated highly oriented pyrolytic graphite (HOPG) samples. Soft XA dichroism spectroscopy is an element specific technique that is sensitive to the magnetic moment of each elemental or chemical species in a complex heterogenous sample. The x-ray energy is chosen such that core level electrons are excited into empty valence states. Using circular polarized x-rays the intensity of the absorption process in a magnetic element depends on the relative orientation between helicity of the x-rays and the magnetic moment of the atom (X-ray magnetic circular dichroism, XMCD)[15]. To obtain an XMCD spectrum two XA spectra with either opposite magnetization or x-ray polarization [16] are recorded and compared. It is important to note that XMCD can provide independent information

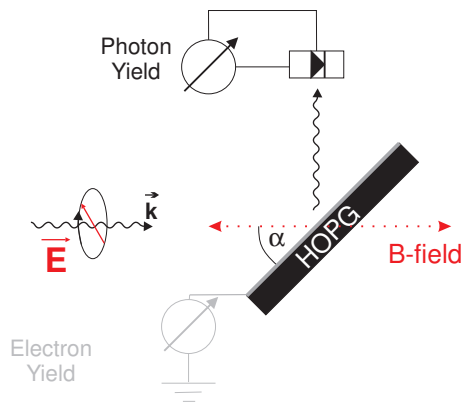


Figure 1. Experimental geometry. Circular polarized x-rays are incident on the sample under an angle α collinear with the direction of the applied magnetic field. A photodiode at 90° to the incoming x-rays can be used to measure the reflected x-ray intensity at $\alpha = 45^\circ$. The absorption yield is measured by monitoring the sample drain current.

about the magnetic order of different elements or even different chemical states of one element in a sample. Furthermore, it is possible to change the depth sensitivity of the approach by using different detection methods for the absorption yield. We will employ exactly these capabilities of XMCD to show that hydrogen atoms at the surface of graphite play a key role in the ferromagnetism of graphite and that the size of the magnetic moment of graphite at the surface can reach the same order of magnitude than classical ferromagnetic materials.

The XA experiments were performed using the eight pole magnet [17] at the elliptical polarized undulator beamline 4.0.2 at the Advanced Light Source in Berkeley [18] at room temperature. The x-ray source provides soft x-rays in the energy range between 250-2000 eV and a typical spectral resolution of $E/\Delta E \approx 5000$ with variable x-ray polarization. The photon energy of the x-ray beam has been calibrated using well known absorption resonances. At the carbon K-resonance the degree of circular polarization of the x-rays emitted by such a device is close to 100%. The electromagnet provides a magnetic field was applied parallel to the direction of the incoming x-rays while the sample was oriented at an angle α as shown in Fig. 1. At $\alpha = 30^\circ$ only the electron yield (EY) emitted from the sample was recorded, while we also recorded the reflected x-ray intensity (reflection yield, RY) at $\alpha = 45^\circ$ using a photodiode. The EY approach provides surface specific information from the first 5-10 nm of the sample [16], while the reflected photons provide more bulk sensitive information (0.1-1 μ m) [19]. XMCD spectra were obtained by switching the direction of the applied field for every data point. The EY and RY data were recorded in an applied field or in remanence after the field was removed.

The two samples discussed in this paper were obtained from a HOPG (0.4 $^\circ$ rocking curve width) bulk sample. Before performing the XMCD measurements we confirmed the negligible amount of magnetic impurities like Fe, Co, Ni by particle induced x-

Sample	Ti	V	Cr	Fe	Co	Ni	Cu	Zn
irr.	3.56	7.1	<0.03	0.25	<0.02	0.11	0.4	0.3
virgin	2.69	8.52	0.11	0.61	$\simeq 0$	0.13	0.06	$\lesssim 0.06$

Table 1. Metallic impurities in the two HOPG samples investigated here measured in ppm = 1 μg element per gram carbon measured by PIXE

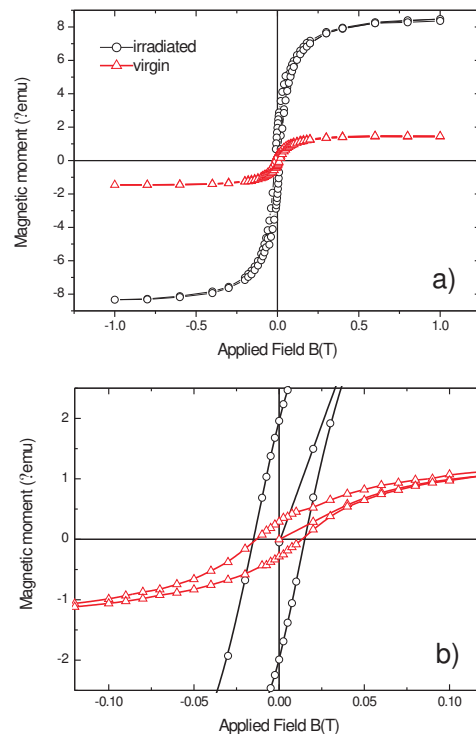


Figure 2. (a) Hysteresis loops (magnetic moment m versus applied field B) measured with SQUID at 300 K for the irradiated (black) and virgin (red) HOPG samples of identical areas and after subtraction of a linear diamagnetic background (field applied \perp c -axis)(b) The low-field region of the hysteresis loop is shown to demonstrate magnetic remanence and coercivity of the two samples.

ray emission (PIXE) and by acquiring XA spectra between 200 eV and 1500 eV. The results of the very sensitive PIXE measurements are summarized in table 1. The total amount of metallic impurities in both samples is of the order of 10 ppm (10 μg per gram carbon), however, the concentration for each of the magnetic elements Fe, Co and Ni is well below 1 ppm. While one sample, in the following referred to as virgin sample, was not treated any further, the other sample was irradiated with a relatively weak fluence of 0.1 $\text{nC}/\mu\text{m}^2$ protons of 2 MeV energy (180 nA ion current). Hysteresis loops of the measured moments from the two samples are shown in Fig. 2. Both hysteresis loops

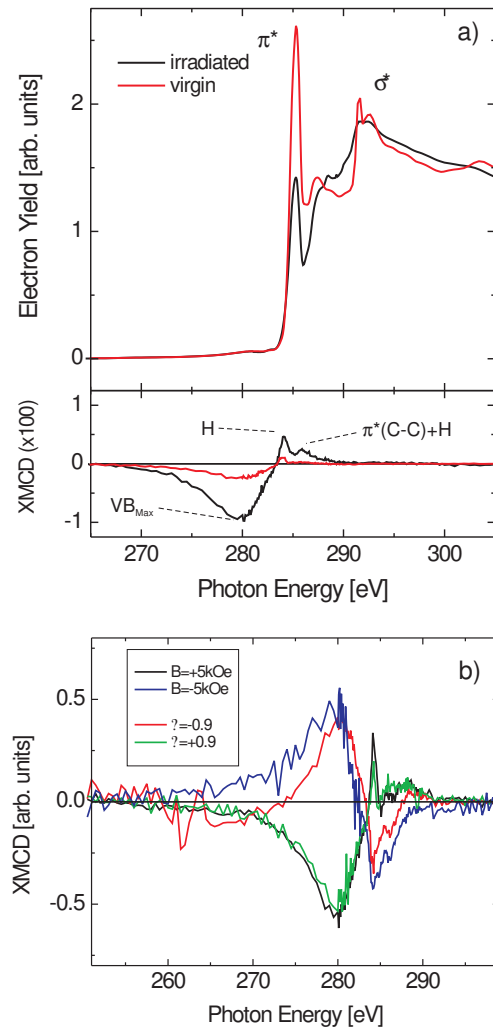


Figure 3. (a) X-ray absorption spectrum of the irradiated (black) and virgin (red) HOPG sample measured using electron yield as well as the XMCD difference (x100) detected using an applied field of ± 0.5 Tesla. (b) Four different XMCD spectra measured by either switching the x-ray polarization or the applied magnetic field for every data point.

show features that are indicative of ferromagnetic order, like magnetic saturation at low fields ($\lesssim 0.5$ Tesla), magnetic remanence at zero field and the existence of a non-vanishing coercive field that is needed to reverse the magnetization into the opposite direction. To illustrate all of these three points we show the overview loops in figure 2(a) as well as magnified view of the low field region of the hysteresis loop in panel (b).

Carbon K-edge soft x-ray absorption spectra of the virgin and irradiated HOPG samples obtained using the electron yield detection at an angle of incidence $\alpha = 30^\circ$ are presented fig. 3(a). The XA spectrum of the virgin sample shows a narrow resonance at 285.3eV and a broader resonance around 293eV, which represent the well known

excitation of 1s core level electrons into empty π^* and σ^* bands [20], respectively. The additional feature at the onset of the σ^* resonance results from an excitonic transition [21]. The π^* and σ^* feature are much broader in the spectra of the irradiated sample and in particular the intensity of the π^* resonance is greatly reduced, a sign that the irradiated sample is more disordered. This observation is consistent with previous microscopy [8] and Raman [22] studies, in which we directly compared irradiated and non-irradiated areas on a carbon sample.

The lower panel in fig. 3(a) shows the XMCD spectrum obtained in an applied magnetic field of ± 0.5 Tesla using circular polarized x-rays. To plot the XMCD difference, which is on average less than 1% of the XA intensity, on the same scale as the XA spectrum we multiplied it by a factor of 100. The excellent signal to noise ratio is achieved by averaging the XMCD difference over several scans. The onset of the absorption yield as well as the XMCD intensity lies well below the π^* -resonance between 270 eV and 275 eV. In our spectra the Fermi level appears at around 283eV, which means that the XMCD and XA signal extend to about 10 eV below E_F . The appearance of magnetic circular dichroism in x-ray absorption below the Fermi level has been previously reported by Mertins *et al.* [23], who have shown that dichroic effects of non-magnetic origin can indeed be observed as low as 270 eV in the Carbon 1s XA spectrum. The broad pre-edge peak of the of the XMCD spectrum in fig. 3 exhibits an absolute maximum at around 3 eV below E_F . The energy range for which the pre-edge XMCD is observed is consistent with the energy spread of the carbon π -bands and the maximum of the XMCD at $\simeq 280$ eV corresponds to the valence band maximum π valence band (VB_{\max}), see for example [24]. The XMCD spectra of both samples also show a positive peak at 284 eV at the onset of the π^* -resonance close to the Fermi level. Previous theoretical investigations predicted the occurrence of a spin polarized band due to H chemisorption [9, 10, 11] at this energy, which we now observe in our XA spectrum. To further convince ourselves that the observed XMCD effects are of magnetic origin we acquired XMCD spectra by either switching the magnetization on each data point (constant x-ray polarization) or by switching the x-ray polarization for each data point (constant field). The four spectra are shown in fig. 3(b). The legend indicates if either the field or the magnetization has been kept constant. No averaging has been applied to these spectra, which explains the higher noise level compared to fig. 3(a). The main features of the XMCD spectra are reproduced in all four spectra and the sign of the peaks is reversed upon either switching the polarization or the magnetization as it is expected for a true intrinsic XMCD effect.

The XMCD spectrum of the irradiated sample shows an additional feature around 286 eV. X-ray studies on single walled carbon nanotubes [25] and graphite surfaces [26] have shown that C-H bond formation will occur through re-hybridization of carbon sp^2 bonds to sp^3 bonds by attachment of hydrogen, leading to a resonance in the XA spectrum about 1 eV above the π^* resonance. We find that both, the hydrogen band as well as the re-hybridized sp^3 carbon π -band exhibit a magnetic moment in the irradiated sample. The sp^3 feature however is absent in the XMCD spectrum of the

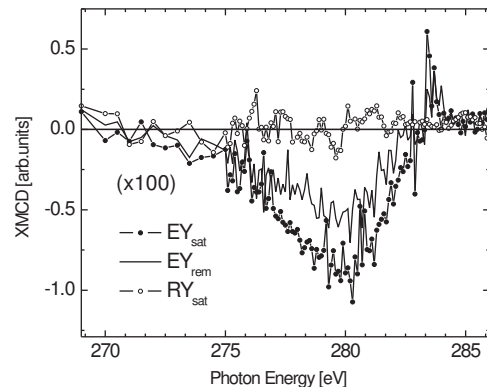


Figure 4. XMCD spectra (x100) of the irradiated HOPG samples obtained using EY in an applied field of ± 0.7 T (\bullet) or in remanence after saturating the sample in a field of ± 0.7 T ($-$). Also shown is the XMCD spectrum acquired in saturation using the reflection yield (\circ). Lines are added as a guide to the eye. All spectra were obtained at $\alpha = 45^\circ$.

virgin sample, while the feature at 284 eV is again a factor of ~ 4 smaller. Combined these observations indicate that the effect of proton irradiation is the incorporation of hydrogen through re-hybridization. This may initially be advantageous for the evolution and stabilization of ferromagnetism in graphite. However, it also becomes evident that intense proton irradiation in particular at ambient temperatures will significantly enhance the diffusion of H and also disturb the crystallographic and hence the electronic structure of graphite reducing the magnetic order. We note that no XMCD intensity is observed at photon energies correlated with the presence of surface oxides around 289eV, excluding the possibility that surface oxidation plays a significant role in the ferromagnetism of graphite.

Figure 4 shows three XMCD spectra (no averaging as in fig. 3(a)) obtained from the irradiated sample. The spectra were acquired at an angle of incidence $\alpha = 45^\circ$, so that the intensity of the RY could be detected at the same time as the EY in our setup. The RY provides bulk sensitive information while the EY is a surface sensitive approach. This is in particular true at energies below the π -resonance where the absorption cross section is small and the x-rays can penetrate deeper into the material, while the escape depth of the secondary electrons contributing to the EY remains small. The XMCD signal acquired using EY shows the prominent feature at 280 eV, which clearly persists after the external field is removed, showing a clear magnetic remanence of about 60% of the saturation value. On the other hand, there is no XMCD detected in the RY spectrum in fig 4. Taking into account the different probing depths of the two approaches (10 nm for EY versus $1 \mu\text{m}$ in RY) we conclude that the observed ferromagnetism in the irradiated sample originates predominantly from the top 10 nm of the sample. Note, that this does not imply that the ferromagnetic order vanishes completely in the bulk of the

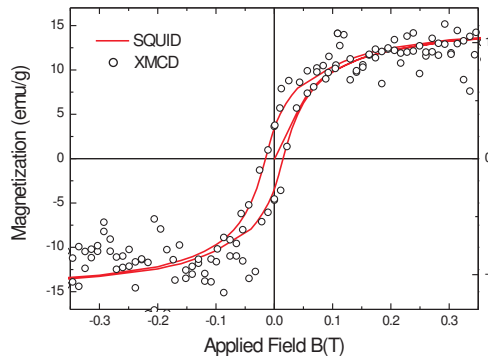


Figure 5. Hysteresis loops of the irradiated sample acquired using SQUID (—) or XMCD (○). The axis on the left side show the magnetization of the sample in emu/g. The axis of the right for the XMCD loop is chosen such that the saturation values coincide for comparison.

sample, instead it means that the (orbital) magnetic moment per atom is smaller than our sensitivity of $10^{-3}\mu_B$.

The information that the majority of the magnetic moment originates from the surface allows us now to estimate the true magnetization values of the HOPG surface by normalizing the magnetic moment obtained by the SQUID hysteresis loop in Fig. 3(a) with the correct thickness. For simplicity we assume a homogeneous distribution of 90% of the magnetic moment within the first 10 nm and we find that the average saturation magnetization for the irradiated sample is of the order of 15 emu/g. Fig. 5 shows the corrected SQUID hysteresis loop displaying the magnetization of the sample surface. For comparison the magnetic moment of Fe is about 220 emu/g or Ni 55 emu/g, which means that the magnetization at the surface of HOPG may reach up to 25% of that of Ni, or on average about $0.1\mu_B$ per C-atom. Note that a direct determination of the total magnetic moment (spin and orbit) of the carbon atoms using x-ray absorption sum rules is not possible because the carbon K-edge XMCD only probes the orbital moment. Nevertheless, both techniques (SQUID and XMCD) measure the same macroscopic magnetic properties. For comparison we show a hysteresis loop obtained using XMCD at a photon energy of 280eV in fig.5 which nicely follows the SQUID hysteresis loop.

In conclusion we report the observation of ferromagnetic order at surfaces of metal free HOPG before and after proton irradiation. The results in virgin HOPG clearly indicate that the observed ferromagnetism in untreated, pure graphite [1] is intrinsic. We find that the observed XMCD signal originates mostly from the near surface region (≈ 10 nm) of the sample where the saturation magnetization may reach up to 25% of that of Ni. The rather large magnetic moment of ferromagnetic HOPG is now consistent with the occurrence of room temperature ferromagnetism. Furthermore, it points toward the possibility that the magnetic properties of carbon can indeed play a significant role in bio-compatible nano-applications as well as an organic magnetic “substrate” in chiral

selective chemistry [27]. The XMCD line shape shows that chemisorbed hydrogen and C-H bond states as well as carbon π -states exhibit a net spin polarization. While the proton irradiation initially increases the magnetic moment by formation of C-H bonds it also disturbs the system for the same reason by introducing disorder and formation of sp^3 -bonds providing an explanation on the limit to which the magnetization in carbon can be increased by ion irradiation. Our results also indicate that hydrogen is not implanted – the implantation probability of 2 MeV photons is very small at the surface – but should come from dissociation of H_2 molecules by the proton irradiation, since a large hydrogen concentration is always present in the near surface region [28].

H.O. would like to thank Joachim Stöhr and Hans-Christoph Siegmann for their support and stimulating discussions. SSRL and ALS are national user facilities supported by the Department of Energy, Office of Basic Energy Sciences. SSRL is operated by Stanford University and ALS is operated by the University of California under contract No. DE-AC02-05CH11231. The work at the University of Leipzig is supported by the DFG under DFG ES 86/16-1 and the European Union project “Ferroc carbon”.

- [1] P. Esquinazi, A. Setzer, R. Höhne, C. Semmelhack, Y. Kopelevich, D. Spemann, T. Butz, B. Kohlstrunk, and M. Lösche. Ferromagnetism in oriented graphite samples. *Phys. Rev. B*, 66:024429–1–10, 2002.
- [2] P. Esquinazi, D. Spemann, R. Höhne, A. Setzer, K.-H. Han, and T. Butz. Induced magnetic ordering by proton irradiation in graphite. *Phys. Rev. Lett.*, 91:227201–1–4, 2003.
- [3] J. Barzola-Quiquia, P. Esquinazi, M. Rothermel, D. Spemann, T. Butz, and N. García. Experimental evidence for two-dimensional magnetic order in proton bombarded graphite. *Phys. Rev. B*, 76:161403(R), 2007.
- [4] H. Xia, W. Li, Y. Song, X. Yang, X. Liu, M. Zhao, Y. Xia, C. Song, T.-W. Wang, D. Zhu, J. Gong, and Z. Zhu. Tunable magnetism in carbon-ion-implanted highly oriented pyrolytic graphite. *Adv. Mater.*, 20:1–5, 2008.
- [5] Y. Kopelevich, R. R. da Silva, J. H. S. Torres, A. Penicaud, and T. Kyotani. Local ferromagnetism in microporous carbon with the structural regularity of zeolite Y. *Phys. Rev. B*, 68:092408–1–4, 2003.
- [6] R. Caudillo, X. Gao, R. Escudero, M. José-Yacaman, and J. B. Goodenough. Ferromagnetic behavior of carbon nanospheres encapsulating silver nanoparticles. *Phys. Rev. B*, 74:214418, 2006.
- [7] N. Parkanskya, B. Alterkopa, R. L. Boxmana, G. Leitusb, O. Berkhc, Z. Barkayd, Yu. Rosenberg, and N. Eliaz. Magnetic properties of carbon nano-particles produced by a pulsed arc submerged in ethanol. *Carbon*, 46:215–219, 2008.
- [8] H. Ohldag, T. Tylicszak, R. Höhne, D. Spemann, P. Esquinazi, M. Ungureanu, and T. Butz. *Phys. Rev. Lett.*, 98:187204, 2007.
- [9] K. Kusakabe and M. Maruyama. Magnetic nanographite. *Phys. Rev. B*, 67:092406–1–4, 2003.
- [10] E. J. Duplock, M. Scheffler, and P. J. D. Lindan. Hallmark of perfect graphite. *Phys. Rev. Lett.*, 92:225502–1–4, 2004.
- [11] O. V. Yazyev. Magnetism in disordered graphene and irradiated graphite. *Phys. Rev. Lett.*, 101:037203, 2008.
- [12] P. Esquinazi, J. Barzola-Quiquia, D. Spemann, M. Rothermel, H. Ohldag, N. García, A. Setzer, and T. Butz. Magnetic order in graphite: Experimental evidence, intrinsic and extrinsic difficulties. *J. Magn. Magn. Mat.* (to be published), see arXiv:0902.1671, 2008.
- [13] X. Yanga, H. Xiab, X. Qinc, W. Lia, Y. Daia, X. Liua, M. Zhaoa, Y. Xiaa, S. Yana, and B. Wangc. Correlation between the vacancy defects and ferromagnetism in graphite. *Carbon*, 47:1399–1406,

- 2009.
- [14] M. Dubman, T. Shiroka, H. Luetkens, M. Rothermel, F. J. Litterst, E. Morenzoni, A. Suter, D. Spemann, P. Esquinazi, A. Setzer, and T. Butz.
 - [15] B. T. Thole, P. Carra, F. Sette, and G. van der Laan. *Phys. Rev. Lett.*, 68:1943, 1992.
 - [16] J. Stoehr and H. C. Siegmann. *Magnetism - From Fundamentals to Nanoscale Dynamics*, volume 152 of *Springer Series in Solid State Sciences*. Springer Heidelberg, 2006.
 - [17] E. Arenholz and S. Prestomon. *Rev. Sci. Instrum.*, 76:083908, 2005.
 - [18] A. Young, E. Arenholz, S. Marks, R. Schlueter, C. Steier, H. Padmore, A. Hitchcock, and D. Castner. *Jour. Synch. Rad.*, 9:270, 2002.
 - [19] See for example: http://henke.lbl.gov/optical_constants/atten2.html.
 - [20] J. Stoehr. *NEXAFS Spectroscopy*, volume 25 of *Springer Series in Surface Science*. Springer, Heidelberg, 1992.
 - [21] P. Brühwiler, A. Maxwell, C. Puglia, A. Nilsson, S. Andreson, and N. Mårtensson. *Phys. Rev. Lett.*, 74:614, 1995.
 - [22] K.-H. Han, D. Spemann, P. Esquinazi, R. Höhne, V. Riede, and T. Butz. Ferromagnetic spots in graphite produced by proton irradiation. *Adv. Mater.*, 15:1719–1722, 2003.
 - [23] H.-Ch. Mertins, S. Valencia, W. Gudat, P. M. Oppeneer, O. Zaharko, and H. Grimmer. Direct observation of local ferromagnetism on carbon in C/Fe multilayers. *Europhys. Lett.*, 66:743–748, 2004.
 - [24] J. Carlisle, S. Blankenshop, L. Termmineello, J. Jia, T. Callcott, D. Ederer, R. Perera, and F. Himpsel. *J. Electron Spectrosc. Rel. Phenom.*, 110:323, 2000.
 - [25] A. Nikitin, H. Ogasawara, D. Mann, R. Denecke, Z. Zhang, H. Dai, K. Cho, and A. Nilsson. *Phys. Rev. Lett.*, 95:225507, 2003.
 - [26] A. Nikitin, L.-A. Näslund, Z. Zhang, and A. Nilsson. *Surf. Sci.*, 602:2575, 2008.
 - [27] R. A. Rosenberg, M. Abu Haija, and P. J. Ryan. *Phys. Rev. Lett.*, 101:178301, 2008.
 - [28] P. Reichart, D. Spemann, A. Hauptner, A. Bergmaier, V. Hable, R. Hertenberger, C. Greubel, A. Setzer, T. Butz, G. Dollinger, D.N. Jamieson, and P. Esquinazi. *Nucl. Instrum. Methods Phys. Res. B*, 249:286, 2006.